Contribution from the Department of Chemistry,
North Carolina State University, Raleigh, North Carolina 27607

Natural Optical Activity of $Co(en)_3^{3+}$ and $Cr(en)_3^{3+}$: Interpretations with Complete Operator Matrices

R. S. EVANS, A. F. SCHREINER,* and P. J. HAUSER

Received January 28, 1974 AIC40060S

An SCC-type, metal AO-optimized molecular orbital model which treats all atoms (M, C, N, H) explicitly is tested and found to relate successfully the absolute configuration of d^3 and d^6 $M(en)_3^{3+}$ to the natural CD of the magnetically allowed $^4T_2$ and $^1T_1$ excitations. The model is tested with complete multicenter operator matrices, **L**, ∇, and **r**, and with successively approximate ones. The CD rotational strength (R) calculations account for (i) the signs of the trigonal components E and A, (ii) the magnitude of $R(^1E)$ of Λ-lel-$Co(en)_3^{3+}$ as known from crystal measurements, (iii) the magnitude of the net activity of the magnetically allowed parent T, and (iv) the sign of this net activity when operators L and r are used. Also, all features but the last one (iv) are accountable when the velocity dipole operator, ∇, is employed in place of the position operator, r. The model also rules out the presence of only the Λ-ob($\lambda\lambda\lambda$) isomer in solutions of Λ-$Co(en)_3^{3+}$ and points to the presence of mostly Λ-lel($\delta\delta\delta$)-$Co(en)_3^{3+}$. On the other hand, the model cannot decide beyond this, *i.e.*, if and how much Λ-ob might be present.

Introduction

Efforts to relate the natural optical activity of transition metal complexes to their absolute configurations at or near the chromophore site have trailed behind the efforts expended in this direction for organic molecules. This situation exists in large part because (i) there are so many more inorganic chromophores, (ii) the large sizes (more atoms, electrons, orbitals) of complexes make it more difficult to derive molecular orbital (MO) coefficients, and (iii) there are greater complexity and expense in evaluating the immense number of operator (orbital angular momentum, $L \equiv L_x + L_y + L_z$, position or distance, $r \equiv x + y + z$, and velocity dipole, $\nabla \equiv \partial/\partial x + \partial/\partial y + \partial/\partial z$) integrals needed to compute the rotational strength, R, by means of the Rosenfeld equation, $R = (e^2/2mc)\mathrm{Im}[\langle a|\hat{M}|j\rangle \cdot \langle j|\hat{L}|a\rangle]$, for which the electric dipole transition moment integral, $\langle a|e\hat{M}|j\rangle$, can be computed by means of either the distance operator or the velocity dipole operator.[1] The present report is only the fourth occasion on which MO's are employed for interpreting the CD of transition metal complexes.

In 1964 Piper and Karipides[2] used a model in which "d-d" excitations, *e.g.*, to $^1T_1$ and $^4T_2$ of $M(en)_3$ ($M = Cr^{III}$ or Co^{III}), obtained rotational strength by borrowing intensity from charge-transfer bands, but crystallographically determined parameters had to be violated in order to make good predictions. The model treats the M-N σ bonds but does not include carbon and hydrogen atoms of the Men rings; *i.e.*, all activity derives from the MN_6 fragment of $M(en)_3$.

Liehr's σ-bonding MO model[3] was contemporary with that of Piper and Karipides. However, its application requires knowledge (very difficult to come by) of the dissymmetric directions of six σ-hybrid orbitals at the nitrogen atoms pointing toward M in $M(en)_3$. In addition, the MN_6 portion of the molecule is treated incompletely, especially the operator matrices, **M** and **L**, by the Liehr and Piper-Karipides models. Nonetheless, the work of a good many chemists[4] was stimulated by the insights of these workers, and this has been nicely summarized by Hawkins.[5]

In 1973 Strickland and Richardson[6] refined the Piper-Karipides MO model by adding the $-CH_2-CH_2-$ portion of each en ligand in the form of a perturbing coulombic field. They included the MN_6 portions of $M(en)_3$ complexes for obtaining their Wolfsberg-Helmholz-like MO's, and the operator matrices include one-center integrals, $\langle\chi_a(M)|\hat{o}|\chi_b(M)\rangle$, and a two-center, $\langle\chi_c(N)|\hat{o}|\chi_d(N)\rangle$, type of integral of this MN_6 segment, where $\hat{o}$ stands for L and the distance operator r.

The MO model of the present paper has the following features: (i) all atoms (M, C, H, N) of $M(en)_3^{3+}$ are treated explicitly; (ii) all atoms are allowed to interact whether they belong to the same or different Men rings, and the interaction is present in the operator matrices, **M** and **L**, and in the MO's; (iii) the electric dipole transition moment matrix, **M**, is constructed completely using the distance, r, and velocity dipole, ∇, operators; (iv) the many-electron-state functions, which are made to be representative of the D_3 point group, are found by avoiding the difficult calculation of energies of states but are constructed, instead, by taking advantage of the properties of the O_h point group

$$\langle {}^4A_{2g}|\hat{L}|{}^4T_{1g}\rangle = 0$$

$$\langle {}^1A_{1g}|\hat{L}|{}^1T_{2g}\rangle = 0$$

(v) multi-ζ metal functions are employed with the 4s and 4p basis orbitals overlap-optimized and orthogonal to the core; (vi) all σ and π M-L and L-L′ interactions are allowed (Strickland and Richardson treated both in their MN_6 fragment); (vii) the semiempirical MO's employed here were derived by an SCC procedure which converges on the charges derived from the density matrix of MO's in an orthonormal Lowdin AO basis. The general nature of this approach makes it suitable for "d-d," charge-transfer, and ligand "internal" excitations. We explore the first of these here.

The use of crystal field models has often been found successful for interpreting the CD activity of "d-d" excitations for $M(en)_3$, and most of these uses have been described and documented in the order of their evolution by Hawkins.[5] The recent efforts by Schaffer,[7] Mason,[8] Richardson,[9] and

(1) H. Eyring, J. Walter, and G. E. Kimball, "Quantum Chemistry," Wiley, New York, N. Y., 1964.
(2) A. Karipides and T. S. Piper, *J. Chem. Phys.*, 40, 674 (1964).
(3) A. D. Liehr, *J. Phys. Chem.*, 68, 665 (1964).
(4) (a) J. Fujita and Y. Shimura in "Spectroscopy and Structure of Metal Chelate Compounds," K. Nakamoto and P. J. McCarthy, Ed., Wiley, New York, N. Y., 1968, Chapter 3, and references therein; (b) R. G. Gillard in "Physical Methods in Advanced Inorganic Chemistry," H. A. H. Hill and P. Day, Ed., Interscience, New York, N. Y., 1968, Chapter 5, and references therein. Also see references in ref 5.
(5) C. J. Hawkins, "Absolute Configuration of Metal Complexes," Wiley-Interscience, New York, N. Y., 1971.
(6) R. W. Strickland and F. S. Richardson, *Inorg. Chem.*, 12, 1025 (1973).
(7) C. E. Schaffer, *Proc. Roy. Soc., Ser. A*, 297, 96 (1968).
(8) S. F. Mason, *J. Chem. Soc. A*, 667 (1971).
(9) F. S. Richardson, *J. Phys. Chem.*, 75, 692 (1971).

Caldwell and Eyring[10] and coworkers of the last expand this list of crystal field approaches, the first of these having used the angular overlap modification. The success of the earlier of these crystal field models depends to some extent on one's outlook; *e.g.*, the 3d–4p mixing of Moffitt[11-13] and Poulet[14] and 3d–4f mixings of Piper and Karipides[13] for $Co(en)_3^{3+}$ nicely predict, on the one hand, opposite signs for ^1E and $^1A_1$ of $^1T_{1g}(t_2^5e^1)$ as observed experimentally, while on the other hand the *net* activity of $^1T_{1g}$ plus $^1T_{2g}$ vanishes, contrary to experiment. The more recent crystal field models[8,9] are worked out along the lines of Tinoco[15] where nonligating groups present themselves as perturbers, and net activity is obtained by these. Of course the ideal model ought to account for the sign *and* magnitude of the *net* activity of spin-allowed, one-electron excitations in addition to predicting the signs and magnitudes of the trigonal components of the magnetically allowed T parent. However, if the latter condition can be met by a bonding model, then it is successful in relating absolute configuration to the CD spectrum given the knowledge of the polarizations of these components from a crystal spectrum containing even the racemate. On the other hand, having a model which can also predict unfailingly the *net* rotational strength of the one-electron, spin-allowed excitations or at least the *sign* of the net activity of the magnetically allowed parent ($^4T_{2g}$ and $^1T_{1g}$ of $Cr(en)_3^{3+}$ and $Co(en)_3^{3+}$, respectively) is a somewhat more ambitious goal. A model of the latter type would free one from even having to know the polarization of components of the magnetically allowed parent. However, it is most realistic at this stage of large-molecule quantum chemistry to search for a general MO model which can relate absolute configuration to the CD signs of trigonal components whose polarizations are known. Here we apply our MO procedure toward $Co(en)_3^{3+}$ and $Cr(en)_3^{3+}$ for excitations to $^1T_{1g}(t_2^5e^1)$ and $^4T_{2g}(t_2^3e^1)$, respectively, although in principle it applies equally well to charge-transfer and ligand internal excitations.

Computational Work

1. **Basis Set and Atomic Orbitals.** The valence orbitals of M (Co or Cr), C, N, and H were chosen to make up the AO basis set of $M(en)_3$, *i.e.*, 3d, 4s, and 4p for M, 2s and 2p for C and N, and 1s for H. From previous experience[16] in this laboratory it was found that the single-ζ orbitals of Clementi and Raimondi[17] are very nearly as good as the double-ζ ones[18] for lighter atoms, *e.g.*, C and N. This conclusion derives from computing two-center and three-center electric dipole moment integrals and overlap integrals.[16] These single-ζ exponents were therefore chosen for the present calculation, and ζ(1s) for H was given[19] the value 1.2. The 3d radial functions of Co^+ were used as given by Richardson, Nieuwpoort, Powell, and Edgell[20] without modification in view of previous experience by Fenske and Radtke.[21] 4s and 4p functions, however, were overlap-optimized for the Co–N bond and made orthogonal to the core orbitals (1s, 2s, 2p, 3s, 3p) of Co as previously given.[20,22] The results are

$$\psi(4s) = -0.02323(\zeta_{1s} = 26.375) + 0.07855(\zeta_{2s} = 10.175) - 0.19388(\zeta_{3s} = 4.690) + 1.01541(\zeta_{4s} = 1.525)$$

$$\psi(4p) = 0.05348(\zeta_{2p} = 11.050) - 0.18667(\zeta_{3p} = 4.385) + 1.01564(\zeta_{4p} = 1.450)$$

The bond distances and angles were taken from the X-ray study of D-$Co(en)_3Br_3 \cdot H_2O$ by Nakatsu[23] and averaging was carried out so as to obtain exact D_3 molecular symmetry. The HCH and HNH dihedral angles (both 109.5°) and the N–H and C–H bond distances (1.02 and 1.09 Å, respectively) were added to this structure. The azimuthal (ϕ) and polar (θ) angles, defined in Figure 1 for the tris chelate ML_6, are 29.8 and 55.0°, respectively. The single-crystal X-ray crystallography of a salt of $Cr(en)_3^{3+}$ has not been published as yet; however, in view of the nearly identical sizes of chromium(III) and cobalt(III) ions[24] and the probably constant "bite size"[25,26] of the ethylenediamine molecule, the same molecular parameters were employed for Λ-lel-$Cr(en)_3^{3+}$ and Λ-lel-$Co(en)_3^{3+}$. Following our very large computer costs for development and detailed computations on $Co(en)_3^{3+}$, the operator matrices of the latter are used for the chromium analog, although MO's of the two ions were still generated separately. This approximation is not serious, since the radial expansions[20,22] of 4s, 4p, and 3d orbitals are similar for Co^+ and Cr^+. lel → ob geometry changes were made by moving C and H atoms.

2. **Molecular Orbitals.** While the AO's of any one atom are orthonormal here, the basis set as a whole is oblique. Therefore, the secular equation $[\mathbf{H} - \mathbf{ES}]\mathbf{C} = \mathbf{0}$ of the oblique set ($\mathbf{S} \neq \mathbf{I}$) has to be cast into standard eigenproblem form, $[\mathbf{M} - \mathbf{E}]\mathbf{T} = \mathbf{0}$, for solution. This can be done by conventional matrix analysis,[27] since the overlap matrix, **S**, is the Hermitian positive-definite metric of the oblique basis. The MO coefficient matrix, **C**, of the oblique AO basis is finally needed in our procedure because we need to transform the operator matrices of the oblique AO basis into MO space.

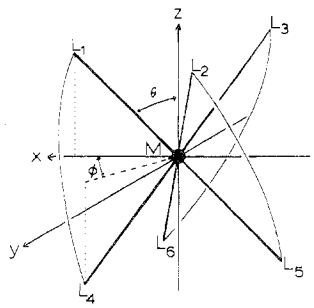

Figure 1. Azimuthal (ϕ) and polar (θ) angles of the tris chelate, ML_6, as measured in the xy plane, the plane of the three C_2 axes; L_1 and L_4 are the two coordinated atoms of one bidentate ligand. The molecular C_3 axis is coincident with the z axis, and θ is the angle between the z axis and the M–L_1, M–L_2, or M–L_3 position vector.

(10) D. J. Caldwell and H. Eyring, "The Theory of Optical Activity," Wiley-Interscience, New York, N. Y., 1971.
(11) W. Moffitt, *J. Chem. Phys.*, **25**, 1189 (1956).
(12) S. Sugano, *J. Chem. Phys.*, 33, 1883 (1960).
(13) T. S. Piper and A. Karipides, *Mol. Phys.*, 5, 475 (1962).
(14) H. Poulet, *J. Chim. Phys.*, 59, 584 (1962).
(15) I. Tinoco, *Advan. Chem. Phys.*, 4, 113 (1962).
(16) R. S. Evans, P. J. Hauser, and A. F. Schreiner, *Inorg. Chem.*, 13, 901 (1974).
(17) E. Clementi and D. L. Raimondi, *J. Chem. Phys.*, 38, 2686 (1963).
(18) E. Clementi, "Tables of Atomic Functions," a supplement to E. Clementi, *IBM J. Res. Develop.*, 9, 2 (1965).
(19) W. E. Palke and W. N. Lipscomb, *J. Amer. Chem. Soc.*, 88, 2384 (1966).
(20) J. W. Richardson, W. C. Nieuwpoort, R. R. Powell, and W. F. Edgell, *J. Chem. Phys.*, 36, 1057 (1962).
(21) R. F. Fenske and D. D. Radtke, *Inorg. Chem.*, 7, 479 (1968).
(22) J. W. Richardson, R. R. Powell, and W. C. Nieuwpoort, *J. Chem. Phys.*, 38, 769 (1963).
(23) K. Nakatsu, *Bull. Chem. Soc. Jap.*, 35, 832 (1962).
(24) L. Pauling, "The Nature of the Chemical Bond," 3rd ed, Cornell University Press, Ithaca, N. Y., 1960.
(25) D. L. Kepert, *Inorg. Chem.*, 11, 1562 (1972).
(26) E. I. Stiefel and G. F. Brown, *Inorg. Chem.*, 11, 434 (1972).
(27) F. E. Hohn, "Elementary Matrix Algebra," 2nd ed, Macmillan, New York, N. Y., 1964.

C will be obtained from the transformation **C** = **PT**, where **T** is easily found since it diagonalizes **M**. In turn, **M** is related to the (known) Hamiltonian matrix, **H**, by **M** = $\mathbf{P}^{-1}\mathbf{HP}$, and $\mathbf{P} = \mathbf{US}^{-1/2}$. The unitary matrix, **U**, of the last equation diagonalizes **S**, and $\mathbf{S}^{-1/2}$ derives[27] from this diagonalized form of **S**. Therefore, once **P** and **T** are derived, one obtains **C** from the equation **C** = **PT**. The inverse, $\mathbf{T} = \mathbf{P}^{-1}\mathbf{C}$, is sometimes termed the Lowdin transformation.[28] A previously based practice for obtaining MO's for large molecules was followed; *i.e.*, the diagonal elements of the Hamiltonian matrix, **H**, for the metal (M) and ligand (L ≡ C, H, N) were taken as $H_{ii}(\mathrm{M}) = -\Sigma_l d_l V_l$ and $H_{ii}(\mathrm{L}) = -(AQ_L^2 + BQ_L + C)$ where V_l is the valence orbital ionization energy (VOIP)[29] of the lth electronic configuration of the metal, and all other constants and features of the procedure are given in ref 29. Off-diagonal elements were obtained by using the Wolfsberg-Helmholz equation[30] with $K = 1.9$. Iterations are carried out until self-consistent charges, Q (Mulliken[31] method using **C**) or Q' (density matrix using T), will result, where for atom A

$$Q_A = Z_A - \sum_k^{\text{mo A}} \sum_i n_k c^2{}_i + \sum_k^{\text{mo A}} \sum_i \sum_{j \neq i} n_k c_{ik} c_{jk} S_{ij}$$

and

$$Q'_A = Z_A - \sum_k^{\text{mo A}} \sum_i n_k t^2{}_{ik}$$

Z_A is the charge of the atomic core and the other symbols in the present notation can be found elsewhere.[32]

3. **Overlap Integrals** ($S_{ij} = \langle \chi_i | \chi_j \rangle$). The overlap matrices, **S**, were obtained by using subroutine INTE (QCPE, Program 82.1) of Yeranos.[33] This subroutine as received from QCPE was made accurate for large internuclear distances and large ζ by extending the number of B functions, $B_k(t)$, to be used for each integral from the fixed number, 10, to such a number, n, so that another term, $B_{n+1}(t)$, would contribute only 10^{-8} or less to the sum of terms preceding it. The routine is the coding of formulas by Kuppermann, Karplus, and Isaacson[34] over single-ζ STO's. Since this subroutine evaluates the integrals in the aligned coordinate system of Figure 2a, it was necessary to express the atomic orbitals of the molecular orbital coordinate system (Figure 2b) as linear combinations of aligned atomic orbitals (Figure 2a); *i.e.*, for the sets of p_m and d_m orbitals in the molecular coordinate system m

$$\mathbf{p_m} = \mathbf{A_p p_a}$$

$$\mathbf{d_m} = \mathbf{B_d d_a}$$

where p_a and d_a are the orbitals in the aligned coordinate system. The transformation matrices **A** and **B** were derived using the Euler angles and Goldstein matrices[35] in the conventional manner. A typical overlap integral of the uth oblique orbital on atom A and the vth orbital on atom B becomes

$$\langle \chi_u(\mathrm{A}) | \chi_v(\mathrm{B}) \rangle = \langle \sum_i a_i \chi'_i(\mathrm{A}) | \sum_j b_j \chi'_j(\mathrm{B}) \rangle$$

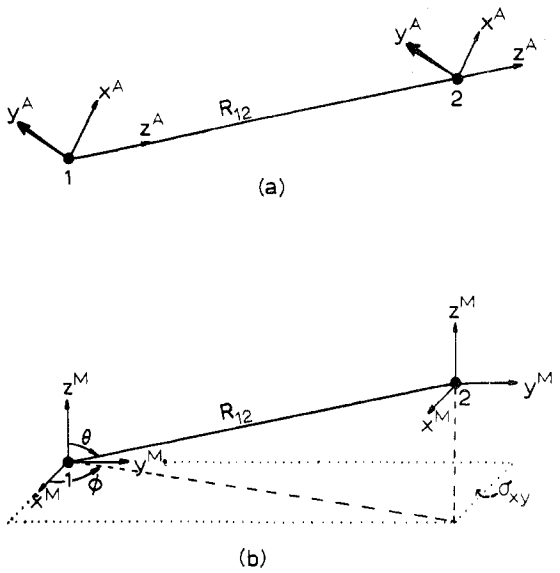

Figure 2. (a) Aligned coordinate system (X^A, Y^A, Z^A) and (b) local molecular coordinate system (X^M, Y^M, Z^M); the two are related by angles θ and ϕ of the figure (see text).

where χ' terms are aligned orbitals computed with INTE.

4. **Distance Integrals**, $\langle \chi_i | \hat{r} | \chi_j \rangle$. The one-center and several, but not all, types of two-center dipole distance integrals were also evaluated with INTE. However, in order to evaluate three-center integrals such as $\langle \chi_i(\mathrm{C}) | \hat{z}(\mathrm{M}) | \chi_j(\mathrm{B}) \rangle$, the operator on the metal center, M, was transformed onto center B. This had the effect of changing every three-center moment integral into a linear combination of two-center integrals. This transformation can be carried out for the general case by recognizing that the coordinates of an electron with respect to center A can also be expressed with respect to those of center B, and the relationship is shown in Figure 3. These coordinates, in fact, are related geometrically by

$$X_A = X_B + R \sin\theta \cos\phi$$

$$Y_A = Y_B + R \sin\theta \sin\phi$$

$$Z_A = Z_B + R \cos\theta$$

where θ, ϕ, and R are defined by the geometry of the complex. An example for which centers M and B are separated by distance R

$$\langle \chi_i(\mathrm{C}) | \hat{x}(\mathrm{M}) | \chi_j(\mathrm{B}) \rangle = \langle \chi_i(\mathrm{C}) | x(\mathrm{B}) | \chi_j(\mathrm{B}) + R \sin\theta \cos\phi \langle \chi_i(\mathrm{C}) | \chi_j(\mathrm{B}) \rangle$$

where B, C, and M are different atoms, is a general statement of this three-center to two-center reduction by these identity transformations.

5. **Velocity Dipole Integrals**, $\langle \chi_i | \hat{\partial}/\partial q | \chi_j \rangle$ ($q = x, y,$ **or** z). The alternative method, which employs the differential operator $\nabla_q = \partial/\partial q$ ($q = x, y,$ or z), was explored for computing electric dipole transition moment integrals in place of the distance operator, $r = x + y + z$. For example, for the z component of transition a → j, one has

$$\langle a | \hat{z} | j \rangle = \frac{-\hbar^2}{m^2 (E_a - E_j)} \langle a | \frac{\hat{\partial}}{\partial z} | j \rangle$$

Using ∇_q in this manner has been termed the velocity dipole procedure, and experimental energy differences were employed here to compute such dipole strengths, D. The integrals of the velocity dipole operator were evaluated by first deriving the analytical functions obtained by operating

(28) P. O. Lowdin, *J. Chem. Phys.*, 18, 365 (1950).
(29) H. Basch, A. Viste, and H. B. Gray, *Theoret. Chim. Acta*, 3, 458 (1965).
(30) M. Wolfsberg and L. Helmholz, *J. Chem. Phys.*, 20, 837 (1952).
(31) R. S. Mulliken, *J. Chem. Phys.*, 23, 1833 (1955).
(32) A. F. Schreiner and T. L. Brown, *J. Amer. Chem. Soc.*, 90, 3366 (1968).
(33) W. A. Yeranos, "INTE," Quantum Chemistry Program Exchange No. 82.1.
(34) A. Kuppermann, M. Karplus, and L. M. Isaacson, *Z. Naturforsch. A*, 14, 311 (1959).
(35) H. Goldstein, "Classical Mechanics," Addison-Wesley, Reading, Mass., 1950.

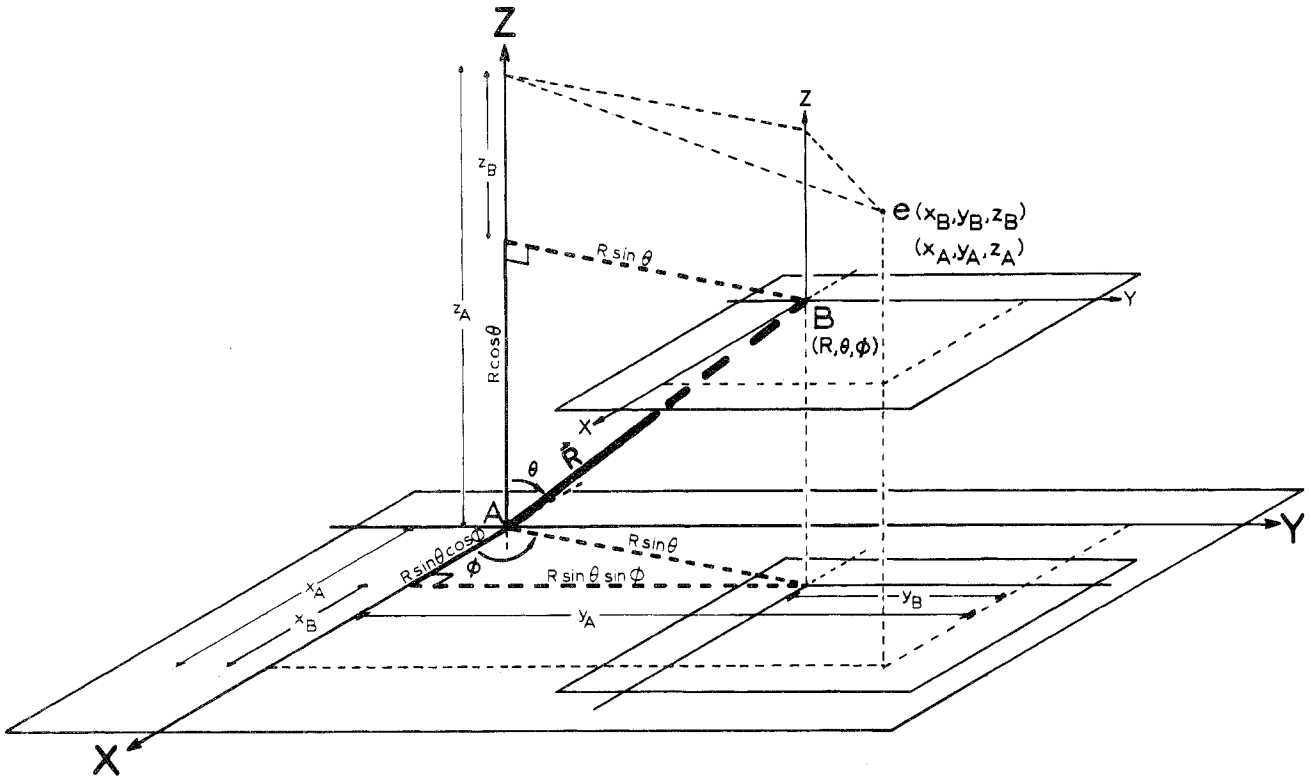

$$X_A = X_B + R \sin\theta \cos\phi$$

$$Y_A = Y_B + R \sin\theta \sin\phi$$

$$Z_A = Z_B + R \cos\theta$$

Figure 3. Position coordinates of an electron with respect to two atoms, A and B.

on the oblique atomic orbital, χ, in the manner, $\hat{\nabla}|\chi\rangle$. This action creates one or several new functions. For example

$$\hat{\nabla}_z(\mathrm{A})|2p_x(\mathrm{B})\rangle = -N_B\zeta_B e^{-\zeta_B r_B}\sqrt{\frac{3}{4\pi}}\left(\frac{X_B Z_B}{r_B}\right)$$

Next, the integration can be carried out; *i.e.*

$$\langle\chi(\mathrm{C})|\hat{\nabla}_z(\mathrm{A})|2p_x(\mathrm{B})\rangle = -\frac{1}{2}\sqrt{\frac{3}{\pi}}N_B\zeta_B\langle\chi(\mathrm{C})|\frac{X_B Z_B e^{-\zeta_B r_B}}{r_B}\rangle =$$

constant × overlap integral

Care is required in the final steps, since the action $\hat{\nabla}|\chi\rangle$ can create strange orbitals like "$2d_{xz}$" of the example here. The orbitals of bra and ket are finally transformed into linear combinations of aligned orbitals recognized by INTE.

6. Orbital Angular Momentum Integrals, $\langle\chi_i|\hat{L}|\chi_j\rangle$. These integrals are a bit easier to formulate once one has worked out the formalism of the velocity dipole operations, $\hat{\nabla}|\chi\rangle$. The procedure for evaluating a nitrogen-metal-carbon three-center integral, J, where $J = \langle 2p_y(\mathrm{N})|\hat{L}_z(\mathrm{Co})|2p_x(\mathrm{Co})\rangle$, is representative and exemplary of the computational steps necessary for constructing the orbital angular momentum matrix, $\mathbf{L}$. First, the operator is transformed from Co to the carbon atom, C. This will have the convenient effect of changing J into a linear combination of two-center integrals. In general, since

$$L_z = i\hbar\left(x\frac{\partial}{\partial y} - y\frac{\partial}{\partial x}\right)$$

needs to be transformed to carbon, C, it is necessary again to know that

$$X_{Co} = X_C + R_{Co-C}\sin\theta\cos\phi$$

$$Y_{Co} = Y_C + R_{Co-C}\sin\theta\cos\phi$$

This follows directly from Figure 3, and the angles are defined by

$$\theta = \cos^{-1}\left(\frac{Z_C - Z_{Co}}{R_{Co-C}}\right)$$

$$\phi = \tan^{-1}\left(\frac{Y_C - Y_{Co}}{X_C - X_{Co}}\right)$$

After substituting these expressions for θ and ϕ into those of X_{Co} and Y_{Co} and putting the explicit form of X_{Co} and Y_{Co} into integral J, one obtains

$$L_z(\mathrm{Co}) = L_z(\mathrm{C}) - i\hbar R_{Co-C}\left\{\sin\theta\left[\cos\phi\frac{\partial}{\partial y(\mathrm{C})} - \sin\phi\frac{\partial}{\partial x(\mathrm{C})}\right]\right\}$$

Substitution of this expression into J then gives

$$J = \langle 2p_y(\mathrm{N})|\hat{L}_z(\mathrm{Co})|2p(\mathrm{C})\rangle =$$

$$-i\hbar\langle 2p_y(\mathrm{N})|X(\mathrm{C})\frac{\hat{\partial}}{\partial y(\mathrm{C})}|2p_x(\mathrm{C})\rangle +$$

$$i\hbar\langle 2p_y(\mathrm{N})|Y(\mathrm{C})\frac{\hat{\partial}}{\partial x(\mathrm{C})}|2p_x(\mathrm{C})\rangle -$$

$$i\hbar R_{Co-C}\sin\theta\cos\phi\langle 2p_y(\mathrm{N})|\frac{\hat{\partial}}{\partial y(\mathrm{C})}|2p_x(\mathrm{C})\rangle +$$

$$i\hbar R_{Co-C}\sin\theta\sin\phi\langle 2p_y(\mathrm{N})|\frac{\hat{\partial}}{\partial x(\mathrm{C})}|2p_x(\mathrm{C})\rangle$$

Next, we operated to the right in each of the four terms so as to create new oblique atomic functions from each operation. The final result is that one can evaluate each of these four terms as a linear combination of overlap integrals. For the integral above we obtain $-0.49783i$ BM when the following input is used.

	Coordinates, Å		
	X	*Y*	*Z*
C	2.75144	−0.51988	0.56800
N	1.42160	−0.81507	1.14661
Co	0.0	0.0	0.0

The carbon and nitrogen orbitals are

$$R(\mathrm{C;p}) = Ne^{-1.5679r}$$

$$R(\mathrm{N;p}) = N'e^{-1.9170r}$$

and the overlap integrals were evaluated with INTE. Other integrals of **L** were evaluated similarly.

7. **Wave Functions of States.** The state functions are constructed in the following manner, using $Cr(en)_3^{3+}$ as an example. Individual determinants, Δ, are written which represent all the possible trigonal electron configurations of octahedral parentage t_{2g}^3 and $t_{2g}^2e_g^1$. The components of Δ are the ground-state and virtual D_3 molecular orbitals, originating from C_3 quantization. The symmetry behavior of these simple determinants, Δ, is then ascertained under the D_3 group operations, C_3 and C_2. This is carried out by operating on the trigonal, C_3-quantized MO's making up these determinants, Δ. Next, the set of determinants, {Δ}, is simply combined so as to construct symmetry functions, Γ, which form representations of point group D_3 in C_3 quantization. Each Γ, of states $^4A_1$ and $^4A_2$ and two sets of ^4E for $Cr(en)_3^{3+}$ is, in fact, a linear combination of determinants, Δ. Finally, it is also necessary to decide how to mix the Γ functions of E states, *e.g.*, $\Gamma(^4E)$ and $\Gamma'(^4E)$, in order to arrive at final state functions $\Psi(^4E,T_1)$ and $\Psi(^4E,T_2)$ whose genealogies are $^4T_1$ and $^4T_2$ of $Cr(en)_3^{3+}$. The above procedure is equally valid for the cobalt analog, recognizing that six-electron, singlet spin states are required for Co(III).

The last step mentioned can be accomplished either by computing state energies,[6] *e.g.*, for $Co(en)_3^{3+}$, $^1E(T_1) < {}^1E(T_2)$, or by evaluating some property[36] clearly to be associated with T_1 or T_2 and admitting that components of these latter constitute the E functions of D_3 symmetry. We followed the second path by making use of the octahedral properties $\langle {}^1A_{1g}|L^{(4)}|{}^1T_{2g}\rangle = 0$ and $\langle {}^4A_{2g}|L^{(4)}|{}^4T_{1g}\rangle = 0$ for $Co(en)_3^{3+}$ and $Cr(en)_3^{3+}$, respectively, where $\mathbf{L} = L_x + L_y + L_z$. For this purpose one again generates operator matrices, $\mathbf{L}_x^{(4)}$, $\mathbf{L}_y^{(4)}$, and $\mathbf{L}_z^{(4)}$, this time using C_4 quantization. Finally, MO's are transformed from C_3 quantization to C_4 quantization, giving the eigenvector matrix $C^{(4)}$ to be used for evaluating the properties named above.

8. **Rotational (*R*) and Dipole (*D*) Strengths.** The rotational strength, $R(a \rightarrow j)$, and dipole strength, $D(a \rightarrow j)$, were computed[10] in dot product manner for transition $a \rightarrow j$, *i.e.*

$$R(a \rightarrow j) = \frac{e^2}{2mc}\mathrm{Im}\{\langle a|\hat{\mathbf{M}}|j\rangle\cdot\langle j|\hat{\mathbf{L}}|a\rangle\}$$

$$D(a \rightarrow j) = e^2\langle a|\hat{\mathbf{M}}|j\rangle\cdot\langle j|\hat{\mathbf{M}}|a\rangle$$

where $\langle \mathbf{M}\rangle$ is the electric dipole transition moment integral divided by e, $\langle \mathbf{L}\rangle$ the magnetic dipole transition moment integral divided by $e/2mc$, and $\mathrm{Im}(g + ih)$ equals h. $\langle \mathbf{M}\rangle$ is evaluated by means of the electronic position, or distance, operator, $r = x + y + z$, or the velocity dipole operator,[1] *e.g.*

$$\langle a|\hat{z}|j\rangle = -\frac{\hbar^2}{m^2(E_a - E_j)}\langle a|\frac{\hat{\partial}}{\partial z}|j\rangle$$

L is the usual orbital angular momentum operator. Our units of R and D are cgs and D^2, respectively.

Results and Discussion

We will first discuss CD results (distance, r, and velocity dipole, ∇, operators) of the magnetic dipole allowed parent excitation, $^1A_{1g}(t_2^6) \rightarrow {}^1T_{1g}(t_2^5e^1)$, for Λ-lel-(+)-$Co(en)_3^{3+}$. The electric dipole strength will then be taken up using operators r and ∇. The possibility of employing more economic, but defective, operator matrices (∇, **r**, and **L**) will also be explored. The rotational and dipole strengths of Λ-ob-$Co(en)_3^{3+}$ will then be compared. Finally, we discuss the rotational and dipole strengths of the magnetically allowed excitation $^4A_{2g} \rightarrow {}^4T_{2g}(t_2^2e^1)$ of the d^3 case Λ-lel-$Cr(en)_3^{3+}$.

The pertinent experimental information about $Co(en)_3^{3+}$ is as follows. From the oriented-crystal, *c*-axis CD spectrum of (+)-$[(Co(en)_3)Cl_3]_2\cdot NaCl\cdot 6H_2O$, as measured by McCaffery and Mason,[37] one has that the rotational strength of the excitation $^1A_1 \rightarrow {}^1E(T_1)$ at 475 nm is 79×10^{-40} cgs. The value of the rotational strength of the second trigonal component of $^1T_1(t_2^5e^1)$, or $^1A_1 \rightarrow {}^1A_2(T_1)$, is at present not measurable in the crystal, since the circularly polarized light would have to traverse a linearly dichroic medium. The energy order[38] of these components is believed to be $^1E < {}^1A_2$. The X-ray structural analyses of D-$[(Co(en)_3)Cl_3]_2\cdot NaCl\cdot 6H_2O$, where D ≡ (+), by Nakatsu, Shiro, Saito, and Kuroya,[39] and D-$[Co(en)_3]Br_3\cdot H_2O$ by Nakatsu[23] clarify that in crystals of the D, or (+), complex, one is working with the Λ-lel conformation. Our calculations are carried out on this lel conformer of the Λ isomer. The solution CD is known to be much weaker than the $^1E(T_1)$ component in the crystal, and Mason measured 4.2×10^{-40} and -0.24×10^{-40} cgs for the rotational strengths of $^1E(T_1)$ and $^1A_2(T_1)$. The CD extrema of these two bands are at 493 and 428 nm but from other crystal measurements of Dingle,[40] Denning,[41] and Dingle and Ballhausen[42] one knows that this ~3-kK separation in the CD is only apparent and much larger than the actual trigonal splitting of $^1T_{1g}$; *i.e.*, the observed room-temperature solution CD spectrum is the net activity of two overlapping bands of opposite sign. The low CD activity of solutions of Λ-$Co(en)_3^{3+}$ may also be the result of this postulated mutual cancelation of the larger activities of ^1E and $^1A_2$ (*vide infra*). This effect is quite commonly encountered in magnetic circular dichroism spectroscopy;[43] *i.e.*, the positive and negative lobes of the Faraday A term in medium fields are separated by hundreds of wave numbers and their heights are small, even though the two Zeeman components giving rise to the A term are much more intense and their energies differ by only ~1 cm^{-1}.

(36) A. Karipides, Ph.D. Thesis, University of Illinois, 1964.

(37) A. J. McCaffery and S. F. Mason, *Mol. Phys.*, 6, 359 (1963).
(38) A. J. McCaffery, S. F. Mason, and R. E. Ballard, *J. Chem. Soc.*, 2883 (1965).
(39) K. Nakatsu, M. Shiro, Y. Saito, and H. Kuroya, *Bull. Chem. Soc. Jap.*, 30, 158 (1957).
(40) R. Dingle, *Chem. Commun.*, 304 (1965).
(41) R. G. Denning, *Chem. Commun.*, 120 (1967).
(42) R. Dingle and C. J. Ballhausen, *Kgl. Dan. Vidensk. Selsk., Mat.-Fys. Medd.*, 35, No. 12, 1 (1967).
(43) A. D. Buckingham and P. J. Stephens, *Annu. Rev. Phys. Chem.*, 17, 399 (1966).

Table I. Rotational Strengths of $^1T_{1g}$ Trigonal Components of Λ-lel-Co(en)$_3^{3+}$ Using Operator Matrices **r** and **L**

Calculation type	$10^{40}R$, cgs ^1E	$^1A_2$	Type of operator matrix
I	50.3	−45.7	Complete
II	80.7	−74.1	All three-center integrals set to zero
III	71.3	−68.5	Only $\langle\chi_{Co}\|\hat{o}\|\chi'_{Co}\rangle$ and $\langle\chi_N\|\hat{o}\|\chi'_N\rangle$ do not vanish
IV	58.5	−53.5	Block diagonal (one block per atom); orbitals of an integral must be on same atom
			Experimental Work
	79		Crystal of (+)-[(Co(en)$_3$)Cl$_3$]$_2$·NaCl·6H$_2$O[a]
	4.2	−0.24	Solution[a]

[a] Reference 37.

The computed results for Λ-lel-Co(en)$_3^{3+}$ can be found in Table I. On using complete operator matrices, **L** and **r**, we predict that the rotational strength of the ^1E trigonal components $R(^1A_1 \rightarrow {}^1E)$ has a value of $+50.3 \times 10^{-40}$ cgs. Thus, the model accounts for the positive sign of $^1E(T_1)$ and approximately for the experimental[37] magnitude ($+79 \times 10^{-40}$ cgs). For the other trigonal component, $^1A_2$, of $^1T_{1g}$ we obtain $R(^1A_1 \rightarrow {}^1A_2) = -45.7 \times 10^{-40}$, on using these complete operator matrices. While the experimental value of R for this second transition (to $^1A_2$) is unknown from crystal data, it is known from the activity of solutions of the Λ isomer that the sign of $R(^1A_1 \rightarrow {}^1A_2)$ is negative, as is computed here. Furthermore, since the net experimental rotational strength for $^1T_1(t_2^5e^1)$ is *ca.* $+4 \times 10^{-40}$ cgs and the net computed R value for $^1T_{1g}$ is $+5.8 \times 10^{-40}$ cgs, the latter value (calculation I, Table I) is in good agreement with the experimental[37] one from the points of view of sign and magnitude. In summary, the MO model, when used with complete operator matrices **r** and **L**, appears to account for (i) the correct signs of rotation for ^1E and $^1A_2$ of $^1T_{1g}$, (ii) the correct sign of the net activity of ^1E plus $^1A_2$ of $^1T_{1g}$, (iii) the approximately correct rotational strength of the measurable component $^1E(T_{1g})$, and (iv) the approximately correct magnitude for the net activity of ^1E plus $^1A_2$ of $^1T_{1g}$.

It is of importance to take notice of the effects on rotational strength when one uses more economic, but defective, operator **r** and **L** matrices by artificially annihilating certain types of integrals contained in complete matrices in order to simplify the calculation. For example, the results of calculation II of Table I are obtained by setting to zero all three-center integrals of operator matrices **L** and **r**. This approximation still gives the right sign and a reasonably good net $^1T_1$ rotational strength (6.6×10^{-40} cgs), but R values for ^1E and $^1A_2$ are overestimated by *ca.* 50% on the basis of results obtained when complete operator matrices (calculation I) are used. Also, the agreement between the computed (80.7×10^{-40} cgs) and experimental (79×10^{-40} cgs) rotational strengths for $^1A_1 \rightarrow {}^1E$ appears to be better than if complete operator matrices are employed (calculation I), which leads to the erroneous conclusion that the D_3 wave functions are very good. Such an error, however, would remain undetected until complete operator matrices are used, as was done here.

In another approximation, the rotational strengths (calculation III, Table I) were obtained by retaining only (i) one-center, $\langle\chi_{Co}|\hat{o}|\chi_{Co}\rangle$, and (ii) one type of two-center integral, $\langle\chi_N|\hat{o}|\chi_N\rangle$, of the seven-atom CoN_6 fragment of Λ-lel-Co(en)$_3^{3+}$. Again, it is found that the net value ($+2.8 \times 10^{-40}$ cgs) of R has the correct sign, as do the trigonal components ^1E and $^1A_2$ but the latter still differ from those of calculation I by *ca.* 40%. Calculation IV is an extension of calculation III in that the operator matrices **L** and **r** of each are block diagonal, but the matrices of calculation IV also include carbon and hydrogen two-center integrals, or $\langle\chi_C|\hat{o}_{Co}|\chi'_C\rangle$ and $\langle 1s_H|\hat{o}_{Co}|1s_H\rangle$. This computational result does not stray far (~15%) from the complete operator calculation (I), so that we recommend the use of incomplete operator matrices **L** and **r** of this particular block-diagonal form for "d-d" transitions. The consequence of this approximation is that three-center integrals need not be evaluated nor the numerous two-center ones of types $\langle\chi_{Co}|\hat{o}_{Co}|\chi'_L\rangle$ and $\langle\chi_L|\hat{o}_{Co}|\chi'_L\rangle$, which involve orbitals from different atoms.

Table II. Rotational Strengths[a] of $^1T_{1g}$ Trigonal Components of Λ-lel-Co(en)$_3^{3+}$ Using Operator Matrices **∇** and **L**

Calculation type[b]	$10^{40}R$, cgs $^1E(T_1)$	$^1A(T_1)$
I	49.5	−53.7
II	32.8	−40.2
III	25.1	−32.3
IV	51.8	−54.3

[a] See Table I for experimental values. [b] See Table I for identification of I-IV.

We now wish to compare the rotational strengths as computed with operators **L** and **r** (Table I) with the ones obtained with operators **L** and **∇** (Table II). When complete operator matrices are evaluated (calculations I) the use of **∇** and **r** for $^1A_1 \rightarrow {}^1E$ leads to nearly identical rotational strengths, *i.e.*, 49.5×10^{-40} and 50.3×10^{-40} cgs, respectively. Excitation to the second trigonal component, $^1A_1 \rightarrow {}^1A_2$, of Λ-lel-Co(en)$_3^{3+}$ is predicted to be of the same negative sign and of about the same magnitude whether **∇** or **r** is used, *i.e.*, -53.7×10^{-40} and -45.7×10^{-40} cgs, respectively. However, the net activity of $^1T_{1g}$, using **∇**, is predicted negative (-4.2×10^{-40} cgs), contrary to what is known from solution experiments.[37] It is most important, nonetheless, that the signs are the same and that the magnitudes of R are quite comparable for excitations to individual trigonal components of the magnetically allowed transition $^1A_{1g} \rightarrow {}^1T_{1g}$.

The consequences of using the approximate operator matrices **∇** and **L** of Table II are similar to what was encountered by using **r** and **L** matrices (Table I). Analogously, it is found that calculation III, in which only the cobalt and nitrogen **L** and **∇** blocks, or $\langle\chi_{Co}|\hat{o}_{Co}|\chi'_{Co}\rangle$ and $\langle\chi_N|\hat{o}_{Co}|\chi'_N\rangle$, are retained, leads to *ca.* 50% deviations (compared to the values obtained by using complete matrices, calculation I) of the rotational strengths of trigonal components, but the use of **r** (calculation III, Table I) leads to overestimates of $|R|$ values, and the use of **∇** (calculation III, Table I) leads to underestimates of $|R|$ values. This behavior makes it dangerous to compute the rotational strengths of very small bands by means of **∇** and calculations of types II or III (Table II). However, the inclusion of all blocks (Co, C, N, H) in the operator matrices so as to account for the one-center and certain two-center expressions (calculation IV, Table II) is quite acceptable, and this is economically important to know. Overall, the use of **r** is recommended over the use of **∇** since the former also predicts the correct net activity of $^1T_{1g}$.

The MO model was also tested by computing the dipole strength of $^1A_1 \rightarrow {}^1T_1$ by means of complete operator matrices **r** and **∇** (calculation I, Table III) or approximate

Table III. Dipole Strengths of $^1T_{1g}$ Trigonal Components of Λ-lel-$Co(en)_3^{3+}$ Using the Distance (r) and Velocity Dipole (∇) Operators

Calculation type[a]	D, D^2 $^1E(T_1)$	$^1A_2(T_1)$	Net $^1T_1$	Operator
I	0.046	0.078	0.124	r
	0.045	0.108	0.153	∇
II	0.066	0.115	0.181	r
	0.011	0.034	0.045	∇
III	0.052	0.098	0.149	r
	0.006	0.022	0.028	∇
IV	0.059	0.102	0.161	r
	0.046	0.105	0.151	∇
			0.12 (exptl[b])	

[a] See Table I for identification of I-IV. [b] Reference 37.

Table IV. Rotational (R) and Electric Dipole (D) Strengths of $^1E(T_1)$ and $^1A_2(T_1)$ of Λ-lel- and Λ-ob-$Co(en)_3^{3+}$ from Complete Operator Matrices[a]

$^1T_1$ (21,322 kK) $^1E(T_1)$	$^1A_2(T_1)$	Conformation
	$10^{40}R$, cgs	
50.3	−45.7	lel
42.7	−42.9	ob
79		Exptl. crystal[b]
4.2	−0.24	Exptl. soln[b]
	D,D^2	
0.046 (0.124)	0.078	lel
0.034 (0.101)	0.067	ob
(0.12)		Exptl.[b]

[a] Complete **L** and **r** operator matrices. [b] Reference 37.

ones (calculations II-IV, Table III) as described above. The estimate of the experimental dipole strengths of $^1T_1$ is 0.12 D^2, and on use of the complete operator matrices **r** and ∇, one obtains 0.124 and 0.153 D^2, respectively. Even though the two computed answers, and especially the first one, are in very good agreement with experiment,[37] they probably overestimate the intensity because our model computes only the static electric dipole contributions to the ^1E and $^1A_2$ intensities, whereas the observed intensity of $^1T_1$ of Λ-lel-$Co(en)_3^{3+}$ probably has vibronic contributions.[40-42]

The use of approximate **r** matrices (calculations II-IV) produces notably smaller dipole strength fluctuations (range 0.149-0.181 D^2) than when approximate ∇ matrices are used (range 0.028-0.151 D^2). Of the three approximate ∇ matrices only the one of calculation IV (0.151 D^2) is near the value 0.153 D^2 of calculation I (complete ∇ matrix). ∇ of calculation IV is block diagonal (Co, C, N, H) as described above. Of the dipole strengths computed with incomplete **r** matrices, the 0.149-D^2 of calculation III (block diagonal in Co and N of (CoN_6) fragment; *vide supra*) and 0.161 D^2 of calculation IV (*vide supra*) are closest to 0.124 D^2 obtained with the complete **r** matrix.

Following the above analysis it was of interest to investigate how skeletal changes of $-CH_2CH_2-$ of each coordinated ethylenediamine in Λ-$Co(en)_3^{3+}$ would influence the rotational strengths and electric dipole strengths of $^1A_1$ and ^1E. Thus, we wish to compare the optical properties of the experimentally known Λ-lel($\delta\delta\delta$)-$Co(en)_3^{3+}$, or Λ-lel(kkk)-$Co(en)_3^{3+}$, of the crystal state, with the other extreme Λ-ob($\lambda\lambda\lambda$)-$Co(en)_3^{3+}$, or Λ-ob(k′k′k′)-$Co(en)_3^{3+}$, of somewhat higher energy.[44] For this purpose we carried out the two computations with complete operator matrices **L** and **r** over all atoms (Co, C, N, H) since the use of **r** accounts reasonably successfully for the features of $^1A_2(T_1)$ and $^1E(T_1)$ of Λ-lel-$Co(en)_3^{3+}$. One notable feature of the lel → ob conformational change is the decrease of the absolute value of the rotational strengths of each trigonal component, ^1E (50.3×10^{-40} to 42.5×10^{-40} cgs) and $^1A_2$ (-45.7×10^{-40} to -42.9×10^{-40} cgs). The second point here is that the decrease of ^1E is greater (15.5%) than the increase of $^1A_2$ (6.1%). One conclusion we draw from this is that the $-CH_2CH_2-$ backbone conversion from lel to ob decreases the CD intensity in a minor, but not negligible, way so that one predicts that the more drastic change of the (CoN_6) skeleton from Λ to Δ structure is actually required to cause a change of the signs of the trigonal components of $^1T_1$. The second conclusion we draw from the present result is that the net integrated $^1T_1$ CD activity of Λ-ob-$Co(en)_3^{3+}$ is expected to be *ca.* zero, since $R(^1A_1 \rightarrow E) = 42.7 \times 10^{-40}$ cgs and $R(^1A_1 \rightarrow {}^1A_2) = -42.9 \times 10^{-40}$ cgs. This does not at all mean that the model predicts no CD bands in the $^1T_1$ region, but it means one ought to see two lobes of opposite sign but same absolute magnitude, very analogous to a pure A term in the Faraday MCD effect.[43] This result rules out the contention that in solutions of the Λ isomer one has 100% Λ-ob. Piper and Karipides argued similarly from an experimental point of view,[45] and Richardson[6] showed very recently that Liehr's MO model applied to the CoN_6 fragment also makes this interesting prediction. However, this attack is not the required strong inference experiment which can rule out the possibility of having a mixture of mostly Λ-lel but some Λ-ob which might give rise to some of the negative CD intensity at 430 nm in the solution of Λ-$Co(en)_3^{3+}$.

The changes of the computed dipole strengths, D, of $^1A_2(T_1)$ and $^1E(T_1)$ as the backbone change in Λ-$Co(en)_3^{3+}$ is made from Λ-lel to Λ-ob closely parallel the changes of the rotational strengths of these components. The lel → ob conversion decreases the intensity of ^1E from 0.046 to 0.034 D^2 and decreases that of $^1A_2$ from 0.078 to 0.067 D^2. In fact, $\sqrt{D(^1E)}$ and $\sqrt{D(^1A_2)}$ decrease by 14.0 and 7.3%, so that the additional insight obtained here is that the decreases of $R(^1E)$ and $R(^1A_2)$ are largely caused by the decreases of the electric dipole transition moment integrals. (See Table IV.)

It was pleasing to discover that the application of the abbreviated but proper three-electron-state functions for Λ-lel-$Cr(en)_3^{3+}$ along with the complete multicenter operator matrices **r** and **L** led to the interpretation of the magnetically allowed excitation $^4A_2(t_2^3) \rightarrow {}^4T_2(t_2^2e^1)$, which is nearly as good as using the six-electron-state functions and the same operators, r and L, for $^1A_1(t_2^6) \rightarrow {}^1T_1(t_2^5e^1)$ of Λ-lel-$Co(en)_3^{3+}$. We show in Table V that the rotational strengths for the one-electron excitations to the trigonal components ^4E and $^4A_1$ are $+13.5 \times 10^{-40}$ and -12.4×10^{-40} cgs, respectively. It is of some surprise that the experimental rotational strength of the ^4E component has not been published, and we are now in the process of measuring this value in crystals.[46] However, the net rotational strength of $^4T_2(t_2^2e^1)$ is known to be $+4.4 \times 10^{-40}$ cgs from solution spectra.[2] The MO model, when used with the complete operator matrices **L** and **r**, yields the reasonable net activity $+1.1 \times 10^{-40}$ cgs, which from the point of view of the sign

(44) E. J. Corey and J. C. Bailar, *J. Amer. Chem. Soc.*, 81, 2620 (1959).

(45) T. S. Piper and A. Karipides, *J. Amer. Chem. Soc.*, 86, 5039 (1964).

(46) R. S. Evans and A. F. Schreiner, work in progress in this laboratory.

Table V. Rotational (R) and Electric Dipole (D) Strengths[a] of $^4E(T_2)$ and $^4A_1(T_2)$ of Λ-lel-Cr(en)$_3^{3+}$

^4E	$^4A_1$	Net $^4T_{2g}$	Operators
	$10^{40}R$, cgs		
13.1	−15.1	−2.0	L, ∇
13.5	−12.4	+1.1	L, r
		+4.4	Exptl. soln[b]
	D, D^2		
0.005	0.014	0.019	∇
0.005	0.009	0.014	r
		0.11	Exptl. soln[b]

[a] Complete operator matrices ∇, L, and r are employed for the computation. [b] Reference 37.

and magnitude is a good result. We might add that the model's underestimate of the rotational strength may actually be in its favor, since the $^4T_2$ CD band intensity is probably vibronic in part and the electric dipole intensity definitely contains vibronic contributions.[47] If, in fact, R of $^4T_2$ were entirely the result of the static mechanism, the underestimate of the computation could then probably be traced to the electric dipole transition moment integral, $\langle ^4A_2|\hat{M}|j\rangle$, of the Rosenfeld equation, $R(^4A_2 \rightarrow j) = \mathrm{Im}\langle ^4A_2|\hat{M}|j\rangle\cdot\langle j|\hat{L}|^4A_2\rangle$, which contains the square root of the dipole strength (*vide infra*). Here, the net dipole strength of $^4A_2 \rightarrow {}^4T_2$ is predicted to be 0.014 D^2 (Table V), which is too small by a factor of 10. Since the model predicts that the rotational strength is too small by a factor of 4, the electric dipole part would largely account for the difference, if it is *assumed* that all the electric dipole character of the dipole strength contributes to the rotational strength. However, the temperature dependence[46] of $R(^4T_2)$ and the real magnitudes of azimuthal (ϕ) and polar (θ) angles need be established first before drawing other conclusions.

Before concluding the discussion of Cr(en)$_3^{3+}$, it is also pointed out that on using the complete velocity dipole matrix, ∇, in place of r one obtains $+13.1 \times 10^{-40}$ and -15.1×10^{-40} cgs for $R(^4E)$ and $R(^4A_1)$, respectively. Thus, the two operators predict nearly the same rotational strength for $^4E(T_2)$, but for $^4A_2 \rightarrow {}^4A_1(T_2)$ operator ∇ predicts a negative R value whose absolute value is 100% larger than predicted by operator r. A similar difference between ∇ and r was encountered for $^1E(T_1)$ and $^1A_2(T_1)$ of Λ-lel-Co(en)$_3^{3+}$ as here; *i.e.*, $R(^1E)$ is nearly invariant, whereas the absolute value of $R(^1A_2)$ is 100% larger when ∇ is used (calculation I, Tables I and II). It is more significant, however, that the signs of rotational strengths of trigonal components ^4E and $^4A_1$ of $^4T_2$ can be computed using either operator, ∇ or r.

It is also worthy of mention that it matters how atomic charges are computed (*vide supra*), if one uses a convergence procedure to self-consistent charges. First, all computations as described above were carried out by using MO coefficients

(47). P. J. McCarthy and M. T. Vala, *Mol. Phys.*, 25, 17 (1973).

Table VI. Rotational (R) and Electric Dipole (D) Strengths of $^1E(T_1)$ and $^1A(T_1)$ of Λ-lel-Co(en)$_3^{3+}$ Using Complete Operator Matrices and MO's from a Mulliken Charge Convergence

$^1E(T_1)$	$^1A_2(T_1)$	Convergence	Operators
	$10^{40}R$,[a] cgs		
513	−391	Mulliken	L, ∇
49.5	−53.7	Lowdin	L, ∇
495	−383	Mulliken	L, r
50.3	−45.7	Lowdin	L, r
	D,[b] D^2		
7.1	9.5	Mulliken	∇
0.045	0.108	Lowdin	∇
6.6	9.1	Mulliken	r
0.046	0.078	Lowdin	r

[a] See Table I for experimental values of R. [b] $D(^1T_1) = 0.12$ D^2.

of self-consistent "Lowdin" charges or

$$Q'_A = Z_A - \sum_k^{\text{mo}} \sum_i^{A} n_k t^2_{ik}$$

(*vide supra*) where t is a component of the eigenvector matrix, **T**, of Lowdin orthonormalized AO's ($[\mathbf{M} - \mathbf{E}]\mathbf{T} = \mathbf{0}$). This procedure was followed because of an earlier discovery in this laboratory that it led to the best set of permanent electric dipole moments for several chromium[16] and manganese complexes. During the present study it was found that the use of molecular orbitals obtained by converging on Mulliken charges (Q_A of "molecular orbitals," *vide supra*) overestimated the dipole strength of $^1T_1$ of Λ-Co(en)$_3^{3+}$ by 2 orders of magnitude (Table VI). This tenfold overestimate of the unsquared electric transition moment integrals entering the dipole strength calculation is also directly responsible for the tenfold overestimate of the net rotational strength of $^1T_1$ (Table VI). The position, r, and velocity dipole, ∇, operators yield very similar dipole strengths and rotational strengths (Table VI). Clearly the MO's of the Mulliken charge convergence predict excited-state electric dipole moments which are 10 times too large. There is perhaps a little less ambiguity about "Lowdin" charges, since one does not arbitrarily divide a quantity such as Mulliken's overlap population, $2C_{ik}C_{jk}S_{ij}$, of the kth singly occupied spin orbital, equally between unlike atoms.

This MO model is now under continued scrutiny to determine if it can account for the CD features of complexes *cis*-M(en)$_2$L$_2$, M(ox)$_3$, and *cis*-M(ox)$_2$L$_2$.

Acknowledgment. Acknowledgment is made to the donors of the Petroleum Research Fund, administered by the American Chemical Society, for support of this research. Several features of this work emerged during the association of A. F. S. with Professor R. G. Denning. P. J. H. was an NDEA predoctoral fellow.

Registry No. Λ-(Co(en)$_3$)$^{3+}$, 27228-84-8; Λ-(Cr(en)$_3$)$^{3+}$, 41509-53-9.